IDEAL FLOW MODELS FOR PALLADIUM MEMBRANE REACTORS

NAOTSUGU ITOH, YUJI SHINDO AND KENJI HARAYA
National Chemical Laboratory for Industry, Tsukuba 305

Key Words: Membrane Reactor, Palladium Membrane, Dehydrogenation, Flow Pattern, Reactor Model

The effects of flow patterns on the dehydrogenation performance of palladium membrane reactors in which a sweep gas is used to remove the permeated hydrogen were examined. By combining two idealized flow patterns, plug and perfect mixing flows, to the reaction and separation streams, five flow models—cocurrent, countercurrent, plug-mixing, mixing-plug, and mixing-mixing models—were analyzed and compared.

It was evident that the countercurrent model leads to the highest degree of conversion and the shortest reactor length requirement while the performance of the mixing-mixing model is the lowest, except when the flow rate of sweep gas chosen is comparatively small. The order of performance among the other three models was dependent on the variables used in calculations.

Introduction

In the previous note[4], it was found experimentally that a palladium membrane reactor can improve the yield of cyclohexane dehydrogenation considerably where the reactor is divided into two parts, i.e., reaction and separation sides, by the palladium membrane. Practical application of such a high-performance reactor to hydrogen-formation reactions is of much interest. However, the type of each part of the rector must be chosen by considering many factors such as rate of reaction, productivity desired,

* Received August 4, 1989. Correspondence concerning this article should be addressed to N. Itoh.

use of datalyst or not, life of catalyst, method of supplying reaction heat and operating conditions. Accordingly, the reactor system[4] proposed, i.e., a catalyst-packed bed for the reaction side and a space mode for the separation side, can not necessarily be said to be the best. For example, if a reaction is very fast, no catalyst will be neeced. In that case, since the ways to provide the heat necessary to the reaction and to unify the reaction temperature become more significant, another type such as a fluidized bed for the reaction side should be rather employed than a packed-bed type. It is postulated that various types of palladium membrane reactor will be usable, whereby the flow of gases through the reactor will be also different.

From this viewpoint, examination of the effect of the flow characteristic of gases on both sides of the palladium membrane reactor on its performance is one of the most important tasks. While there are simulation studies[7-9] that compare the performance of cocurrent and countercurrent operations, mainly for microporous membrane reactors, no attempt for a specific case like a palladium membrane reactor has been made to examine the effect on conversion of the extent of fluid mixing on both sides. On the other hand, several studies[1-3, 10-12] on modeling the flow in a membrane gas separator have been made, using idealized flow patterns such as plug and perfect mixing flows. Although it cannot give a strict description of the flow behavior occuring in the separator, such a method has been able to present valuable information necessary to evaluate its performance. Therefore, a similar approach to obtaining a primary understanding of the palladium membrane reactor was employed. The objective of this study is to make clear the effects of the flow patterns on the performance of the palladium membrane reactor by using several ideal flow models.

1. Ideal Models for Flow Pattern in the Palladium Membrane Reactor

Plug and perfect-mixing flows are known to be simple and easily understandable flow patterns to describe the flow behavior in a reactor. Plug flow has no axial or radial mixing diffusion, while in perfect-mixing flow all constituent gases are completely mixed with one another. Considering combinations of two such flow patterns for the streams of the reaction and separation sides, there are five models as shown in **Fig. 1.** In each model, the lower and upper parts of the membrane reactor correspond to the reaction and separation sides respectively. Both the cocurrent and countercurrent models assume plug flow on both sides of the membrane.

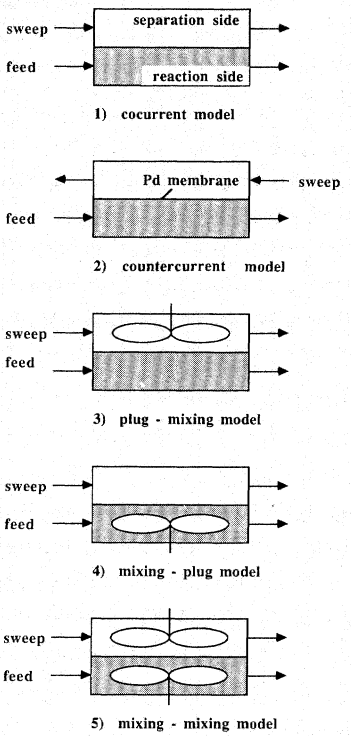

Fig. 1. Ideal flow models in the palladium membrane reactor

2. Development of Basic Equations for Five Models

By assuming isothermal and steady-state conditions in the whole reactor and no pressure drop along the reactor length, basic equations were derived. With regard to hydrogen permeation through a palladium membrane, the Sieverts law[5] was assumed to be applicable. According to this law, the permeation rate of hydrogen under steady-state conditions, Q_H, is given as follows.

$$Q_H=(DC_0A/t_m)(\sqrt{\pi_{Hr}}-\sqrt{\pi_{Hs}}) \quad (1)$$

where π_{Hr} and π_{Hs} are dimensionless partial pressures of hydrogen on the reaction and separation sides respectively. In general, the dehydrogenation reaction can be expressed as follows.

$$C \rightleftharpoons D+mH_2$$

where m is the stoichiometric coefficient of hydrogen generated and is usually in the range 1–3.

2.1 Cocurrent model

In this case, the sweep gas flows in the same direction as the feed gas. By taking the material balance over the difference reactor length, dL, the following set of ordinary differential equations can be obtained.

$$dU_C/dL=-Da\cdot f \quad (2)$$

$$dU_H/dL=Da\cdot f-Tu(\sqrt{\pi_{Hr}}-\sqrt{\pi_{Hs}})/m \quad (3)$$

$$U_D=1-U_C \quad (4)$$

$$V_H = 1 - U_C - U_H \tag{5}$$

where U_i and V_i are dimensionless flow rates of gas i in the reaction-side and separation-side streams respectively. Da is the Damköhler number, Tu introduced in this study is a dimensionless parameter representing the ratio of the hydrogen permeation rate to the feed rate, and f is a rate expression depending on the kind of reaction selected. The above simultaneous equations are numerically solved as an initial-value problem with initial conditions as follows.

$$L=0: U_c=1.0,\ U_D=U_H=V_H=0$$
$$U_I=U_I^0,\ V_I=V_I^0 \tag{6}$$

2.2 Countercurrent model

Although the flow of the sweep gas is opposite to the direction to the feed, one can derive basic equations analogous to those for the cocurrent model, i.e., Eqs. (2)–(4). Equation (5) must be replaced by the following equation.

$$V_H = U_H + V_H^e - (1 - U_C) \tag{7}$$

where V_H^e is the flow rate of hydrogen at the outlet of the separation side. The initial and boundary conditions become

$$L=0: U_C=1,\ U_D=U_H=0,\ V_H=V_H^e,\ U_I=U_I^0 \tag{8}$$

$$L=1: V_H=0,\ V_1=V_I^0 \tag{9}$$

Since V_H^e is unknown initially, it must be assumed and then the set of equations are numerically solved as an initial-value problem. This trial-and-error method is continued until the boundary condition, i.e., $V_H=0$ at $L=1$, is satisfied. In practical calculations, when the following relation holds, the calculation is completed.

$$|\{V_H^e(\text{ass.}) - V_H^e(\text{cal.})\}/V_H^e(\text{ass.})| < 1\times10^{-5} \tag{10}$$

V_H^e (cal.) can be obtained by the reverse calculation from the values at $L=1$ using Eq. (7).

2.3 Plug-mixing model

Let us consider a model in which the flow on the reaction side is plug flow and the flow on the separation side is perfect mixing. In this case, the concentration of hydrogen on the separation side is regarded as constant anywhere in this stream. Basically, Eqs. (2)–(4) can be also applied to this model after replacing π_{Hs} by π_{Hs}^e (constant).

Numerical integrations were carried out by assuming V_H^e (ass.), and the results were compared with V_H^e (cal.), which is calculated from the solutions, U_C^e and U_H^e, using the following material balance at the outlet.

$$V_H^e = 1 - U_C^e - U_H^e \tag{11}$$

2.4 Mixing-plug model

This model is the reverse of the plug-mixing model. The composition of the reaction-side stream is regarded to be identical with that at the outlet. Therefore, the material balance on the reaction side can be written using the outlet values (U_C^e, U_D^e and U_H^e) as follows.

$$U_C^e = Da\cdot f^e \tag{12}$$

$$U_D^e = 1 - U_C^e \tag{13}$$

$$U_H^e = 1 - U_C^e - V_H^e \tag{14}$$

Since f^e can be represented as a function of U_C^e, U_D^e and U_H^e, these equations are solved as a system of simultaneous equations in three unknowns even if V_H^e (ass.) is assumed. The change in flow rate of hydrogen in the separation-side stream can be written by the following differntial equation.

$$dV_H/dL = Tu(\sqrt{\pi_{Hr}^e} - \sqrt{\pi_{Hs}})/m \tag{15}$$

V_H^e (cal.) thus obtained is compared with V_H^e (ass.) using Eq. (10), and if the criterion is satisfactory, the calculation is finished.

2.5 Mixing-mixing model

In this model, since the composition of each side stream of the membrane reactor is uniform at any instant of time, they are regarded as identical with those in the exit stream from the reactor. Therefore, the following equation is added to Eqs. (12)–(14), and they are solved as a system of four simultaneous equations in four unknowns.

$$V_H^e = Tu(\sqrt{\pi_{Hr}^e} - \sqrt{\pi_{Hs}^e})/m \tag{16}$$

where π_{Hr}^e and π_{Hs}^e are respectively given using U_i^e and V_i^e as

$$\pi_{Hr}^e = (P_r/P_0)mU_H^e/(U_C^e + U_D^e + mU_H^e + U_I^0) \tag{17}$$

$$\pi_{Hs}^e = (P_s/P_0)mV_H^e/(mV_H^e + V_I^0) \tag{18}$$

To calculate the above basic equations a concrete expression for f is needed, so dehydrogenation of cyclohexane to benzene was taken as a model reaction ($m=3$). According to the previous kinetic study[5], f is given as follows.

$$f = \frac{(K_P/P_0^3)(\pi_C/\pi_H^3) - \pi_D}{(P_r/P_0)\{1 + (K_D K_P/P_0^2)(\pi_C/\pi_H^3)\}} \tag{19}$$

where K_D and K_P are 1.16×10^{-4} Pa^{-1} and 2.33×10^{11} Pa^3 respectively. On the assumption that $P_r=P_s=P_0$, the simultaneous ordinary differential equations developed above were numerically integrated by the Runge-Kutta-Gill method. The simultaneous non-linear algebraic equations were solved by the Brent method.

3. Results and discussion

3.1 Conversion and hydrogen concentration profiles

Figures 2—6 show the conversion and hydrogen concentration profiles along the reactor length for the five models. In Fig. 2, the conversion curve corresponding to a conventional catalytic reactor ($Tu=0$) is also shown. The curve shows that there exists a reaction equilibrium beyond which the reaction can never proceed at all.

With regard to the difference in hydrogen concentration between the reaction and separation sides throughout the reactor, that of the countercurrent model is found to be the largest among the models considered. This means that the amount of hydrogen removable from the reaction side to the separation side is the largest.

3.2 Comparison of reactor performance

Figures 7–9 compare the performance attainable by each reactor model with varying parameters. With V_I^0 taken as X-axis, the ratio of the flow rate of the sweep gas to that of the feed has a great effect on the coversion since it relates closely to the amount of hydrogen removable from the reaction side: the lager the value of V_I^0, the larger is the amount of hydrogen removed. Figure 7 shows the calculation result when both Da ($=300$) and Tu ($=300$) are large; this means that the rates of both reaction and hydrogen permeation are comparatively large. The performance of the models is found to be larger in the order: countercurrent > cocurrent ≒ plug-mixing > mixing-plug > mixing-mixing. While the performance of the countercurrent model is absolutely large, there are only small differences among the other four models. Since it is considered that the reactor that can achieve higher conversion with smaller V_I^0 is more excellent, the countercurrent model, by which 100% conversion is obtained with around $V_I^0=35$, is concluded to be best.

The intermediate case, where Da and Tu are decreased to 50 and 150 respectively, is shown in Fig. 8. The results are similar to those seen in Fig. 7. However, the differences among the conversions by the models other than the countercurrent one are found to be a little larger. Here, it must be noted that the conversion curve of the countercurrent model crosses that of the cocurrent one near $V_I^0=10$, i.e., the performance of the former becomes a little inferior to that of the latter. This can be explained as follows.

Figure 10 shows the conversion and the hydrogen concentration profiles for both the cocurrent and countercurrent models when $V_I^0=5$. In the case of the countercurrent model, just after the reactant enters the reactor the permeation of hydrogen always takes place in the direction from the separation to the reaction side. This is simply because the hydrogen

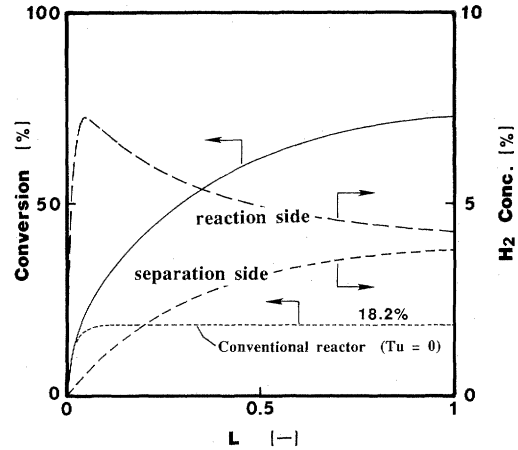

Fig. 2. Conversion and hydrogen concentration profiles along the reactor length for the cocurrent model ($Da=100$, $Tu=30$, $U_I^0=4$, $V_I^0=50$)

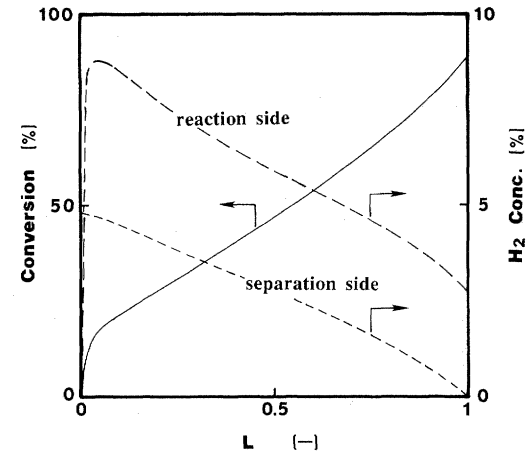

Fig. 3. Conversion and hydrogen concentration profiles along the reactor length for the countercurrent model ($Da=100$, $Tu=30$, $U_I^0=4$, $V_I^0=50$)

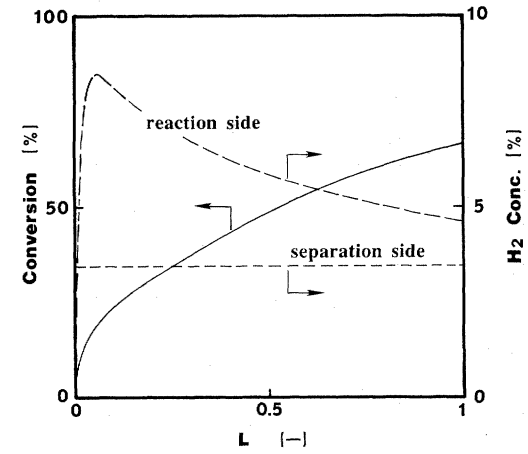

Fig. 4. Conversion and hydrogen concentration profiles along the reactor length for the plug-mixing model ($Da=100$, $Tu=30$, $U_I^0=4$, $V_I^0=50$)

concentration on the separation side is higher than that on the reaction side. Such a phenomenon, i.e., reverse permeation, plays a role in decreasing the rate

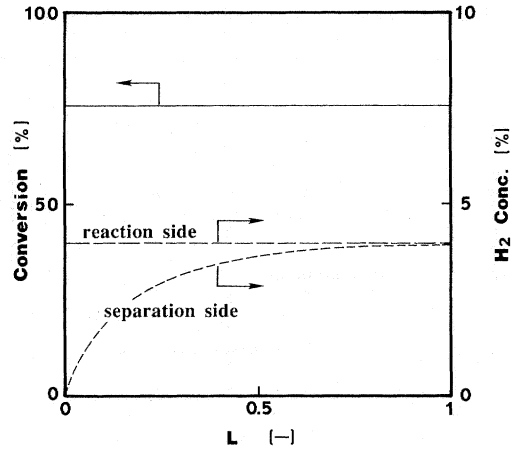

Fig. 5. Conversion and hydrogen concentration profiles along the reactor length from the mixing-plug model ($Da=100$, $Tu=30$, $U_I^0=4$, $V_I^0=50$)

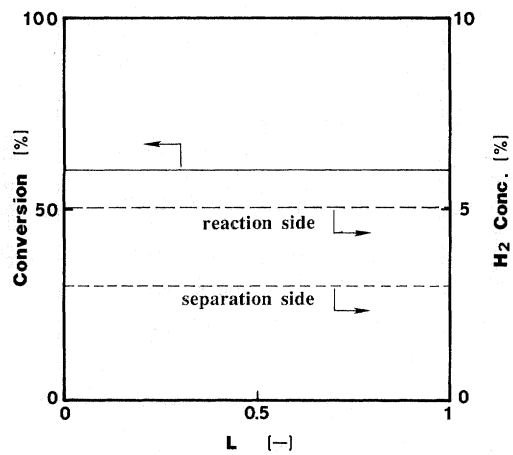

Fig. 6. Conversion and hydrogen concentration profiles along the reactor length for the mixing-mixing model ($Da=100$, $Tu=30$, $U_I^0=4$, $v_I^0=4$, $v_I^0=50$)

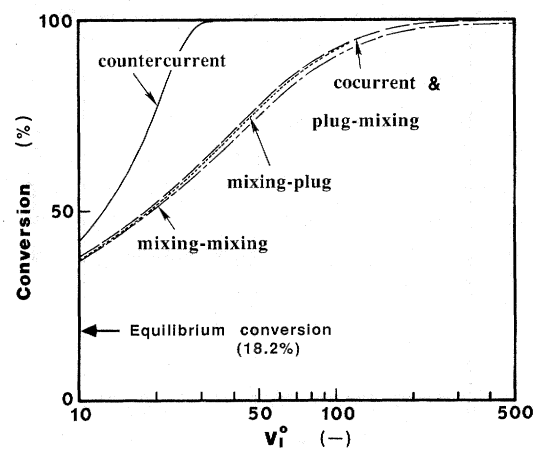

Fig. 7. Comparison of reactor performance calculated for the five models ($Da=300$, $Tu=300$, $U_I^0=4$)

of reaction since the presence of hydrogen in unfavorable for dehydrogenation in terms of reaction kinetics as well as chemical equilibrium. Accordingly, the initial rise in the conversion curve of the

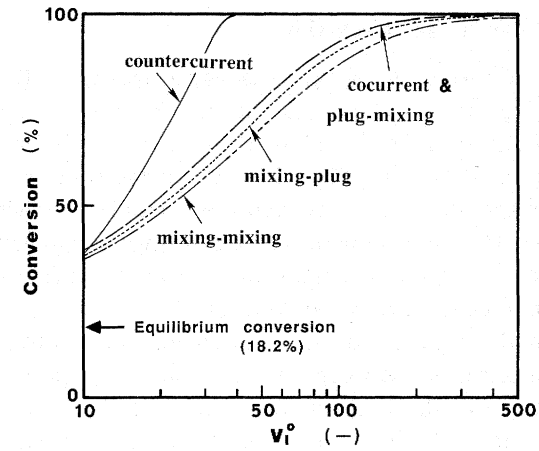

Fig. 8. Comparison of reactor performance calculated for the five models ($Da=50$, $Tu=150$, $U_I^0=4$)

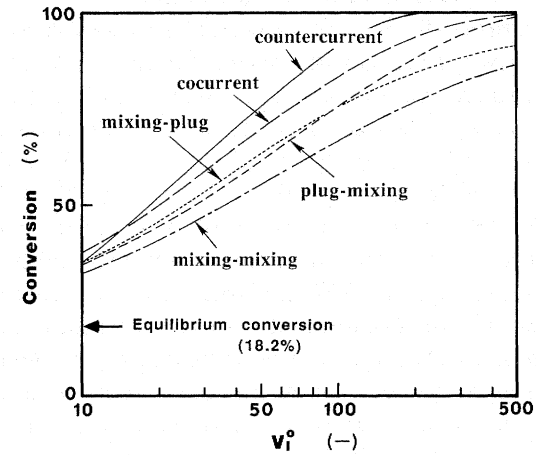

Fig. 9. Comparison of reactor performance calculated for the five models ($Da=20$, $Tu=30$, $U_I^0=4$)

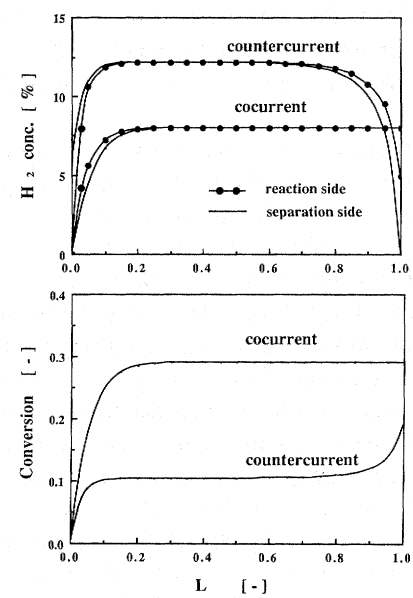

Fig. 10. Conversion and hydrogen-concentration profiles for the cocurrent and countercurrent models when V_I^0 is small ($Da=50$, $Tu=150$, $U_I^0=4$, $V_I^0=5$)

countercurrent model is found from Fig. 10 to be much smaller than that of the cocurrent model. The reaction, however, will be accelerated by the start of hydrogen removal from the reaction field as soon as the hydrogen concentration on the reaction side exceeds that on the separation side. As V_I^0 is decreased, the concentration of hydrogen (the amount of hydrogen permeated) in the separation-side stream will increase more quickly and will be nearly balanced with that in the reaction-side stream. As a result, further increase in conversion will be impossible before the reaction-side stream meets the sweep gas with lower or zero concentration of hydrogen around its outlet. On the other hand, in the cocurrent model nothing mentioned above occurs around the inlet of the reaction, so that the conversion increases without suppression by reverse permeation and can exceed that of the countercurrent model.

The results when still smaller values for *Da* and *Tu* were chosen have a different tendency compared with the above two cases as shown in Fig. 9. Still, the countercurrent model results in the highest conversion except in the region less than $V_I^0 = 14$, similarly to that in Fig. 8. The mixing-mixing model also remains in the lowest position, similarly to the cases in Figs. 7 and 8. The most different point is that the order between the plug-mixing and the mixing-plug models changes according to the flow rate of sweep gas, V_I^0. Below $V_I^0 = 100$, the latter is found to outperform the former. This can also be explained by the reason as mentioned above; it is due to the reverse permeation of hydrogen from the separation to the reaction side around the inlet of reactor as can be easily understood by comparing the hydrogen concentration profiles in Figs. 4 and 5.

Conclusion

Ideal flow models for a palladium membrane reactor consisting of reaction and separation sides separated from each other by a palladium membrane were proposed to evaluate the effects on its dehydrogenation performance of flow patterns on the reaction and separation sides. Five reactor models considered on the basis of combinations of two idealized flow patterns—plug and perfect mixing flows—were compared: cocurrent, countercurrent, plug-mixing, mixing-plug and mixing-plug models.

It was found that the countercurrent model shows the highest performance while the mixing-mixing model shows the lowest except when a small flow rate of sweep gas is chosen. The order of performance among the other three models (mixing-plug, plug-mixing and cocurrent models) was dependent on the variables used in calculations.

Nomenclature

A	=	membrane area	[m^2]
C_0	=	hydrogen concentration dissolved in palladium membrane at a temperature T_0 and a pressure P_0	[$mol \cdot m^{-3}$]
D	=	diffusion coefficient of hydrogen in palladium membrane	[$m^2 \cdot s^{-2}$]
Da	=	Damköhler number for reaction side at T_0 and P_0, $k_r v_r^e P_r / u_C^0$	[—]
f	=	rate expression	[—]
k_r	=	rate constant of dehydrogenation	[$mol \cdot m^{-3} \cdot s^{-1} \cdot Pa^{-1}$]
K_D	=	adsorption equilibrium constant	[Pa^{-1}]
K_P	=	equilibrium constant for dehydrogenation	[Pa^3]
l	=	reactor length	[m]
l_0	=	total length of reactor	[m]
L	=	dimensionless reactor length, l/l_0	[—]
m	=	stoichiometric coefficient	[—]
p_i	=	partial pressure of gas i	[Pa]
P_r	=	total pressure on reaction side	[Pa]
P_s	=	total pressure on separation side	[Pa]
P_0	=	reference pressure, 1.01325×10^5	[Pa]
t_m	=	thickness of membrane	[m]
Tu	=	dimensionless parameter representing the ratio of hydrogen permeation rate to feed rate, $DC_0A/(t_m u_C^0)$	[—]
u_i	=	flow rate of gas i in reaction-side stream	[$mol \cdot s^{-1}$]
u_C^0	=	flow rate of reactant at reaction-side inlet	[$mol \cdot s^{-1}$]
U_i	=	dimensionless flow rate of gas i in reactionside stream, u_i/u_C^0, $u_H/(mu_C^0)$	[—]
U_i^e	=	U_i value at outlet	[—]
U_i^0	=	U_i value at inlet	[—]
v_i	=	flow rate of gas i in separation-side stream	[$mol \cdot s^{-1}$]
v_r^e	=	reaction-side volume	[m^3]
V_i	=	dimensionless flow rate of gas i in separation-side stream, v_i/u_C^0, $v_H/(mu_C^0)$	[—]
V_i^e	=	V_i value at outlet	[—]
V_i^0	=	V_i value at inlet	[—]
π_i	=	dimensionless pressure, p_i/P_0	[—]

〈Subscripts〉

C	=	reactant of dehydrogenation
D	=	dehydrogenated product
H	=	hydrogen
i	=	gas i
I	=	inert gas
r	=	reaction side
s	=	separation side

〈Superscripts〉

0	=	inlet value
e	=	outlet value

Literature Cited

1) Blaisdall, C. T. and K. Kammermeyer: *Chem. Eng. Sci.* **28**, 1249 (1973)
2) Haraya, K., K. Obata, T. Hakuta and H. Yoshitome: *Sep. Sci. Technol.*, **23**, 305 (1988)
3) Hwang, S. T. and K. Kammermeyer: "Membranes in Separations," Wiley, New York (1975)

4) Itoh, N.: *AIChE Journal*, **33**, 1576 (1987)
5) Itoh, N., H. Tanabe, Y. Shindo and T. Hakuta: *Sekiyu Gakkaishi*, **28**, 323 (1985)
6) Lewis, F. A.: "The PALLADIUM HYDROGEN System," p. 94, ACADEMIC PRESS, London (1967)
7) Mohan, K. and R. Govind: *Sep. Sci. Technol.*, **23**, 1715 (1988)
8) Mohan, K. and R. Govind: *Ind. Eng. Chem. Res.*, **27**, 2064 (1988)
9) Mohan, K. and R. Govind: *AIChE Journal*, **34**, 1493 (1988)
10) Pan, C. Y.: *AIChE Journal*, **29**, 545 (1983)
11) Shindo, Y., T. Hakuta, H. Yoshitome and H. Inoue: *Sep. Sci. Technol.*, **20**, 445 (1985)
12) Stern, S. A. and W. P. Walawender, Jr.: *Sep. Sci. Technol.*, **20**, 445 (1985)